

Two-dimensional photonic crystals for mid-infrared quantum dot intersublevel emission

Julien Houel¹, Estelle Homeyer¹, Xavier Checoury¹, Stephane Laurent¹, Guy Fishman¹, Sebastien Sauvage¹, Philippe Boucaud^{1,2}, Stephane Guilet², Remi Braive², Audrey Miard², Aristide Lemaitre², and Isabelle Sagnes²

¹ Institut d'Electronique Fondamentale, Batiment 220, CNRS Univ Paris Sud, 91405 Orsay, France

² Laboratoire de Photonique et de Nanostructures, Route de Nozay, 91406 Marcoussis, France

Received 23 April 2008, revised 1 October 2008, accepted 28 October 2008

Published online 14 January 2009

PACS 42.70.Qs, 42.72.Ai, 78.30.Fs, 78.30.-j, 78.67.Hc

* Corresponding author: e-mail philippe.boucaud@ief.u-psud.fr, Phone: +33-1-69154092, Fax: +33-1-69154090

We have fabricated two-dimensional photonic crystals for the mid-infrared spectral range. These photonic crystals are engineered in order to show optical modes in resonance with quantum dot intersublevel transitions. A novel fabrication technique was developed to obtain suspended membranes in a planar geometry. The membranes are 3 μm thick and the lat-

tice periodicities vary between 3.5 μm to 6.5 μm . We show that the photonic crystals modes can be probed by the room temperature emissivity using a photomodulation technique. Bloch-modes of the photonic crystals are observed around 11 μm wavelength.

© 2009 WILEY-VCH Verlag GmbH & Co. KGaA, Weinheim

1 Introduction Doped semiconductor quantum dots exhibit optical transitions called intersublevel transitions which cover the mid- to far-infrared spectral range. Numerous studies have been devoted to the physics of intersublevel transitions over the past years. Linear absorption measurements involving bound-to-continuum and bound-to-bound transitions have been reported [1, 2]. The strong coupling regime for the electron–phonon interaction has been evidenced by magnetoabsorption experiments [3]. The formalism associated with the formation of mixed electron–phonon quasiparticles called polarons has been shown to adequately describe the dynamics properties of quantum dots [4, 5]. Nonlinear properties, electronic intersublevel structure and mid-infrared quantum dot photodetection have been also investigated [6]. Recently, mid-infrared intersublevel absorption of a single quantum dot has been observed and spatially resolved at the tens of nanometer scale [7]. Fewer works have been devoted to the mid-infrared emission properties of intersublevel transitions [8]. As compared to intersubband emission of quantum wells, the self-assembled quantum dots naturally exhibit in-plane polarized transitions which can in turn lead to normal incidence emission. The observation of spontaneous emission remains however a difficult task because of

the weak radiative efficiency in the mid-infrared due to the efficient non radiative relaxation. One way to circumvent this problem is to control the optical density of states in structures with embedded quantum dots. This engineering can lead to better coupling to the radiative modes and in turn to a better emission and collection efficiencies. One way to control the optical density of states is to use two-dimensional photonic crystals [9]. In the mid-infrared, two-dimensional photonic crystals have been implemented on top of quantum well based quantum cascade structures in order to achieve emission from the surface [10]. Two-dimensional photonic crystals following the membrane approach in a planar geometry have not been reported in this spectral range. Photonic crystal quantum cascade lasers were recently demonstrated using a focused ion beam fabrication technique [11] but in this latter work, the air hole axis was in the quantum well plane.

In this work, we report on the fabrication of two dimensional photonic crystals for the mid-infrared spectral range. We describe the fabrication techniques to obtain 3 μm thick GaAs membranes following a planar geometry. We show that the optical modes can be probed by the room temperature emissivity using a photomodulation technique. This method is original since it does not require an internal

source like quantum dots or the coupling of an external source. The room temperature “gray-body” emission of the GaAs membrane is sufficiently spectrally large to probe the photonic crystals around 7–20 μm wavelength.

2 Two-dimensional photonic crystal fabrication

The photonic crystals were fabricated on GaAs substrates. A reference sample was first grown by organometallic chemical vapor deposition (MOCVD). Similar samples containing InAs quantum dot layers were grown by molecular beam epitaxy [7]. For the MOCVD sample, an AlGaAs stop-etch layer containing 80 percent of aluminium was first deposited on the GaAs substrate. A 3 μm thick GaAs layer was then epitaxially grown on it. The sample was covered by a 7 μm thick oxide layer deposited by plasma-enhanced chemical vapor deposition. This was followed by the deposition of Ti/Au and In/Au metallic layers. Thanks to these metallic layers, the sample was then bonded on a second handle GaAs substrate. The substrate of the first wafer was removed by wet chemical etching down to the AlGaAs stop etch layer. The photonic crystals were then patterned by e-beam lithography following a triangular lattice. The lattice periodicity was varied between 3.5 μm to 6.5 μm . Circular air columns were then etched down to the oxide layer by inductively coupled plasma etching. In the final step, the oxide layer was removed by wet etching in fluorydric acid, leaving a suspended GaAs membrane. Figure 1 and 2 show a top view and a cross-section scanning electron micrograph images of the fabricated photonic crystals. Figure 1 shows an hexagonal H2 microcavity. Figure 2 shows the GaAs suspended membrane which is separated from the substrate by a 7 μm thick air gap. The advantage of the process is to provide membranes with a good mechanical stability on a thick GaAs substrate. The symmetry of the structure avoids the coupling between quasi-TE and quasi-TM modes. The 3 μm thickness of the GaAs layer corresponds to a $\lambda/2n$ thickness for a 20 μm wavelength. The air hole radius is around $0.35a$ where a is the lattice periodicity. The number of periods are around 10 in order to take advantage of the

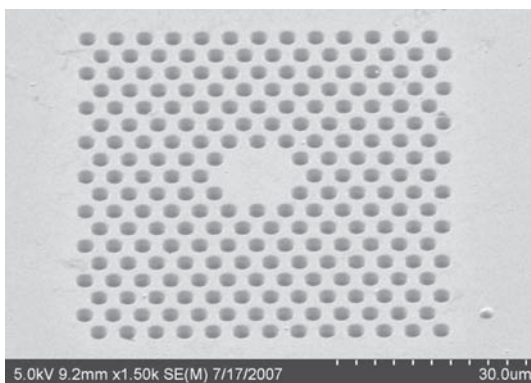


Figure 1 Top view by scanning electron micrograph of a H2 hexagonal cavity obtained with a two-dimensional photonic crystal triangular lattice.

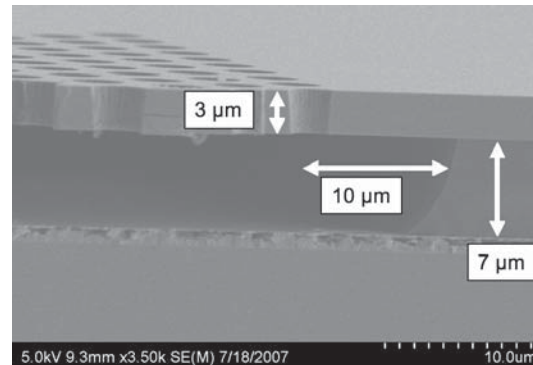


Figure 2 Cross-section scanning electron micrograph of the GaAs photonic crystal membrane. The bonding metallic layer is observed at the interface between the air gap and the GaAs substrate.

photonic crystal effect while keeping a good mechanical stability for the membrane.

3 Reflectivity measurements The properties of the photonic crystals were first calculated using standard plane wave techniques. Considering the structural parameters, a photonic band gap is predicted in TE polarization between $u = a/\lambda \approx 0.28$ and $u = 0.38$ in normalized frequency. The TE polarization corresponds to the in-plane polarization of the S–P intersublevel transitions [2]. Confined optical modes appear in the photonic band gap for hexagonal cavities. The signature of the confined modes can be obtained by performing reflectivity measurements with an illumination of the top surface. For this purpose, we have used a Fourier-transform infrared spectrometer coupled to an infrared microscope equipped with $\times 15$ Cassegrain mirrors. There is no light illumination at normal incidence with Cassegrain mirrors. The infrared microscope allows to spatially select a small spatial region in the reflectivity spectrum. Figure 3 shows the room temperature reflection spectra for three H2 photonic crystal cavities, as shown in Fig. 1 characterized by different lattice parameters. The spectra are dominated by Fabry–Perot resonances associated with the 3 μm thick GaAs membrane. Superimposed on the Fabry–Perot resonances, a reflectivity dip is clearly observed at 778 cm^{-1} , 715 cm^{-1} and 656 cm^{-1} for lattice periodicities varying from 4.5 μm to 5.5 μm . This dip shifts to lower energy as expected as the lattice parameter increases. Its amplitude corresponds to a change of reflection around 40%. Its linewidth is around 8 cm^{-1} corresponding to a quality factor $Q = \omega/\Delta\omega \approx 100$. The spectral position of this dip remains constant in normalized frequency at a value of $u = a/\lambda \approx 0.35$ as expected from the scaling law of photonic crystals. It corresponds to a resonant cavity mode confined by the in-plane photonic band gap of the structure which is evidenced here by near-normal incidence reflection measurements.

4 Emissivity measurements The optical properties of the photonic crystals can also be probed by emissivity

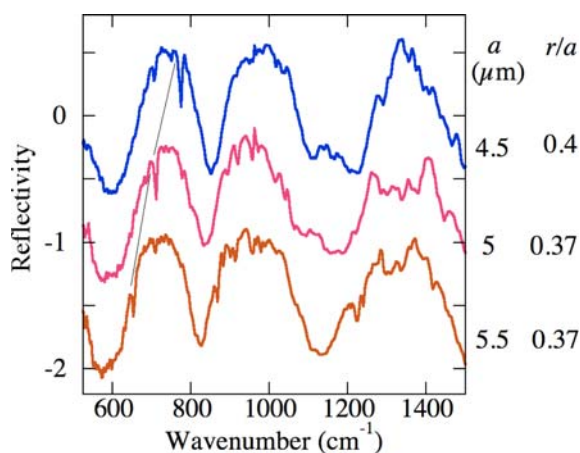


Figure 3 (online colour at: www.pss-b.com) Reflectivity of the H2 cavities as observed in Fig. 1. The lattice periodicities and air hole radius ratio are indicated on the right. The curves have been offset for clarity. Besides the Fabry–Perot oscillations, a reflectivity dip is observed from top to bottom at 778 cm^{-1} , 715 cm^{-1} and 656 cm^{-1} .

measurements. As the investigated spectral range lies between $5\text{ }\mu\text{m}$ and $20\text{ }\mu\text{m}$, one can use the “gray-body” emission of the material at room temperature. Standard emissivity measurements require to heat the sample at elevated temperatures in order to separate the sample contribution from the residual room temperature background. Another approach is to modulate the emissivity properties of the structure by an interband optical excitation. We have thus introduced a new technique based on the photomodulation of the emissivity of the photonic crystals. The sample is placed in the emission port of a Fourier transform infrared spectrometer. The photonic crystal structure is illuminated by an optical excitation provided an argon ion laser. The incident optical power chopped at low frequency is a few milliwatt. This optical excitation is fully absorbed by the GaAs membrane. If necessary, the excitation can be tightly focused in order to optically excite only the hexagonal cavity. The change of emissivity is recorded with a lock-in amplifier synchronized at the chopping frequency. This signal is then redirected to the spectrometer acquisition board. The spectrometer is operated in step-scan mode, thus allowing to achieve a good signal to noise ratio. The signal amplitude depends on the incident optical power and chopping frequency. Meanwhile the spatial resolution of the photomodulation recorded with a small size mercury cadmium telluride photodetector depends on the illumination spot size convoluted by thermal and carrier diffusions. For a thin slab, the emissivity at a given frequency is given by the ratio of the optical power per unit area emitted in solid angle $d\Omega_k$ and the optical power per unit area emitted by a blackbody at the same temperature. From Kirchoff’s law, the emissivity is thus given by $\xi_k(\omega) = 1 - R_k(\omega) - T_k(\omega)$ where R and T are the reflectance and transmittance of the film [12]. The power spectrum of the film is then given by the product of the emis-

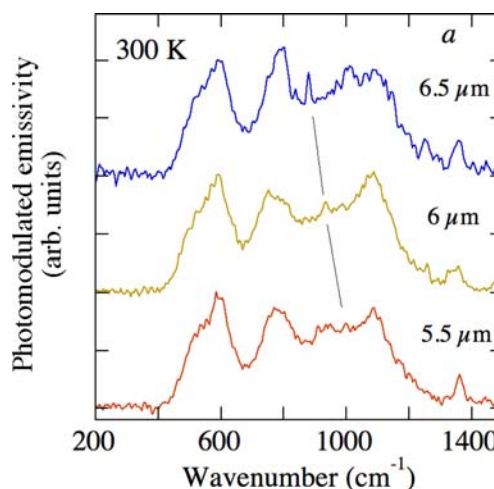


Figure 4 (online colour at: www.pss-b.com) Photomodulated room temperature emissivity of three photonic crystals with different lattice periodicities indicated on the right hand side of the image. The measurement is performed on a structure containing a H1 cavity. Superimposed on top of the membrane emissivity, resonant peaks which shift with the lattice periodicity can be observed from top to bottom at 880 cm^{-1} , 930 cm^{-1} and 1000 cm^{-1} corresponding to a normalized frequency of 0.565.

sivity times the same temperature Planck blackbody power spectrum. In the photomodulation emissivity measurements, the photogenerated carriers change the free carrier absorption of the material and its temperature. It modifies therefore the emissivity and the local changes are recorded by the lock-in amplifier. The measured signal must also take into account the instrument response including the beam splitter transmission and the detector response.

Figure 4 shows a comparison of the photomodulated emissivity spectra for three different photonic crystal lattices ($6.5\text{ }\mu\text{m}$, $6\text{ }\mu\text{m}$ and $5.5\text{ }\mu\text{m}$). The measurement is performed on a sample containing a H1 cavity. The broad resonances correspond to the change of emissivity of the membrane convoluted by the Planck law, independently of the photonic crystal pattern. We observe on top of these broad resonances a narrow resonance around 880 cm^{-1} , 930 cm^{-1} and 1000 cm^{-1} which shifts to high energy as the lattice periodicity decreases. The normalized frequency associated with this optical mode is ≈ 0.565 . The quality factor of the mode is around 70. Two features can explain the difference in the linewidth between reflectivity and emissivity measurements: the angles of incidence for emission and reflection are different; in emissivity measurements, the photo-induced free carriers generate additional losses through free-carrier absorption. Such modes are observed at the same energy on two-dimensional photonic crystal membranes without cavity or on samples with H2 cavities. They correspond to a Bloch mode of the photonic crystal, i.e. an optical mode spatially delocalized over the photonic crystal structure, and not a resonant defect cavity mode. It can be coupled from the surface towards the ra-

diative continuum through the k wvector components above the light cone. We emphasize that the measured signal is integrated over several crystal periods. The spatially delocalized modes have a stronger field overlap with the internal gray-body source, which explains in turn that they are more easily observed than the cavity modes. This measurement demonstrates that the photonic crystal Bloch modes can be probed in the mid-infrared spectral range by room temperature photomodulated emissivity measurements.

5 Conclusion We have reported a novel fabrication technique to obtain two-dimensional photonic crystal membranes in a planar geometry for the mid-infrared spectral range. Self assembled quantum dots can be embedded in these photonic crystal membranes. We have shown that the optical modes of the photonic crystals can be probed using the photomodulation of the room temperature emissivity of the crystals. Bloch modes of the photonic crystals have been evidenced by this technique. The next step will consist in the investigation of the low temperature quantum dot photoluminescence in resonance with cavity or photonic crystal modes. One difficulty of such measurement with an internal source in the mid-infrared will be associated with the weak radiative efficiency of the intersublevel emission even at low temperature.

Acknowledgement This work was supported by French National Research Agency ANR-PNANO program QUOCA.

References

- [1] S. Sauvage, P. Boucaud, F. H. Julien, J. M. Gerard, and V. Thierry-Mieg, *Appl. Phys. Lett.* **71**(19), 2785–2787 (1997).
- [2] F. Bras, P. Boucaud, S. Sauvage, G. Fishman, and J. M. Gerard, *Appl. Phys. Lett.* **80**(24), 4620–4622 (2002).
- [3] S. Hameau, Y. Guldner, O. Verzelen, R. Ferreira, G. Bastard, J. Zeman, A. Lemaître, and J. M. Gérard, *Phys. Rev. Lett.* **83**(20), 4152–4155 (1999).
- [4] S. Sauvage, P. Boucaud, R. P. S. M. Lobo, F. Bras, G. Fishman, R. Prazeres, F. Glotin, J. M. Ortega, and J. M. Gerard, *Phys. Rev. Lett.* **88**(17), 177402 (2002).
- [5] E. A. Zibik, L. R. Wilson, R. P. Green, G. Bastard, R. Ferreira, P. J. Phillips, D. A. Carder, J. P. R. Wells, J. W. Cockburn, M. S. Skolnick, M. J. Steer, and M. Hopkinson, *Phys. Rev. B* **70**(16), 161305 (2004).
- [6] P. Boucaud and S. Sauvage, *Comptes Rendus Physique* **4**(10), 1133–1154 (2003).
- [7] J. Houel, S. Sauvage, P. Boucaud, A. Dazzi, R. Prazeres, F. Glotin, J. M. Ortega, A. Miard, and A. Lemaître, *Phys. Rev. Lett.* **99**(21), 217404 (2007).
- [8] S. Sauvage, P. Boucaud, T. Brunhes, A. Lemaître, and J. M. Gerard, *Phys. Rev. B* **60**(23), 15589–15592 (1999).
- [9] E. Yablonoitch, *Phys. Rev. Lett.* **58**(20), 2059–2062 (1987).
- [10] R. Colombelli, K. Srinivasan, M. Troccoli, O. Painter, C. F. Gmachl, D. M. Tennant, A. M. Sergent, D. L. Sivco, A. Y. Cho, and F. Capasso, *Science* **302**(5649), 1374–1377 (2003).
- [11] M. Lončar, B. G. Lee, L. Diehl, M. A. Belkin, F. Capasso, M. Giovannini, J. Faist, and E. Gini, *Opt. Express* **15**(8), 4499–4514 (2007).
- [12] C. M. Cornelius and J. P. Dowling, *Phys. Rev. A* **59**(6), 4736–4746 (1999).